

# Fluid-structure interaction model of fish schooling in a rectangular pattern

Rose Gebhardt

December 13, 2021

## Abstract

This project was intended to replicate and validate Daghooghi and Borazjani's paper [1]. In their paper, a three-dimensional model of a rectangular school of mackerel with varying lateral distance between fish were simulated to observe the hydrodynamic benefits of schooling. The simulation was used to find the steady-state velocity of the swimmers and the resulting thrust force, power and efficiency. Additionally, flow visualizations were shown to compare the wakes of swimmers in different formations. In this project, the thrust power and efficiency were first computed analytically using the Lighthill model [2] and compared to the results found by Daghooghi and Borazjani. Next, a two-dimensional model was created using the same schooling formations and swimming motion as the original. Flow visualizations were then created with the intent to compare the wakes of the 2D simulations with the 3D simulations. Finally, a two-dimensional model of a single swimmer was simulated with and without viscous effects considered to verify the validity of the inviscid assumption. **All relevant code and video outputs can be found at this GitHub repository.**

## Project Description

### Fish Dynamics

The exact geometry of a mackerel could not be found in literature, but the 2D cross-section of a fish is often modelled by an airfoil or hydrofoil [1] [3], so the baseline shape of the mackerel was defined by a symmetric elliptical airfoil [4] whose length,  $L$ , was normalized to one.

To match the experimentally found kinematics for a typical mackerel, wave propagation through the fish is defined by  $y(x, t) = a(x) \sin(kx - \omega t)$  where the amplitude of the undulatory motion is defined by the second-order polynomial  $a(x) = 0.02 - 0.08x + 0.16x^2$ . This leads to a maximum oscillation amplitude of  $a_{max} = 0.1$  at the end of the tail [5]. The wave propagation was defined by the wave number  $k = 2\pi/\lambda$ , with the wavelength  $\lambda = 0.95L$ , and the angular frequency  $\omega = 2\pi f$ , with the characteristic frequency  $f$  defined by the Reynolds number and Strouhal number.

A typical mackerel swimming Reynolds number and Strouhal number are [5]

$$Re = \frac{UL}{\nu} = 50000$$

$$St = \frac{2fa_{max}}{U} = 0.25$$

Using the kinematic viscosity of water  $\nu = 1 \text{ mm}^2/\text{sec}$ , these values provide the swimming velocity  $U$  and the angular frequency  $\omega$ . For simulations with multiple mackerel, it is assumed that all the fish are swimming in-phase.

## Analytical Model Results

In Daghooghi and Borazjani's paper, the swimming velocity was found by simulating the 3D fish schooling model until the swimmer reached a steady-state velocity [1]. The analytical calculations assume a constant swimming velocity without any interference from other fish. To validate Daghooghi and Borazjani's results, the power and efficiency were computed using the Lighthill model and compared to their results found numerically.

Lighthill's elongated body theory was used to compute the cycle-averaged energy transfer and the rate of energy transfer. This is a reaction force propulsion model, where the forces are assumed to be primarily due to the acceleration caused by added mass. For these calculations, let  $U$  be the longitudinal velocity,  $V = \frac{\omega}{k}$  be the speed of the wave propagation, and  $W$  be the cycle averaged lateral velocity at the tail. Using  $w$ , the velocity of the water due to the motion of the tail segment and  $m_a$ , the added mass of the tail based on the diameter at  $x = 0.8L$ , we can derive  $P_{\text{total}}$ ,  $P_{\text{wake}}$ ,  $P_{\text{thrust}}$  and the Froude propulsive efficiency,  $\eta_f$ , with the equations below [6]:

$$\begin{aligned} w &= W \left( \frac{V - U}{V} \right) \\ m_a &= \frac{1}{4} \pi \rho d^2 \\ P_{\text{total}} &= m_a w U V \\ P_{\text{wake}} &= \frac{1}{2} m_a w^2 U \\ P_{\text{thrust}} &= m_a \left( w W U - \frac{1}{2} w^2 U \right) \\ \eta_f &= \frac{P_{\text{thrust}}}{P_{\text{total}}} = 1 - \frac{1}{2} \left( \frac{V - U}{V} \right) \end{aligned}$$

These values were evaluated to  $P_{\text{total}} = 4.813 \times 10^{-3}$  W,  $P_{\text{wake}} = 2.2885 \times 10^{-3}$  W,  $P_{\text{thrust}} = 2.5428 \times 10^{-3}$  W and  $\eta_f = 0.5263$ . These results are tabulated and compared to Daghooghi and Borazjani's results below:

Model	Velocity $U_0$ ( $U$ )	Cycle averaged thrust power ( $P_{\text{thrust}}$ )	Froude efficiency ( $\eta_f$ )
$w = 0.3L$ Pattern	$1.045 U_0$	$0.950 \times 10^{-3}$	0.297
$w = 0.4L$ Pattern	$1.009 U_0$	$0.930 \times 10^{-3}$	0.290
$w = 0.7L$ Pattern	$0.940 U_0$	$0.934 \times 10^{-3}$	0.292
$w = 1.0L$ Pattern	$0.927 U_0$	$0.917 \times 10^{-3}$	0.292
$w \rightarrow \infty$ Pattern	$0.869 U_0$	$0.945 \times 10^{-3}$	0.269
Lighthill Model	$1.000 U_0$	$2.5428 \times 10^{-3}$	0.526

The cycle-averaged thrust power found analytically was larger than those found by Daghooghi and Borazjani. The 2D model does not perfectly match the 3D model so it is expected that these values might vary, but, as expected, these values are on the same order of magnitude.

On the other hand, the Froude efficiency values were unexpected. The efficiency of the schooling fish should have been larger than that of a single swimmer and they should have been larger than 0.5 (assuming  $U$  and  $V$  act in the same direction). This may indicate that the Froude efficiency was defined differently by Daghooghi and Borazjani.

## Simulation Results

To visualize the wake for the two-dimensional models, the resulting pressure fields were found using queen 2.0, a MATLAB based GUI for computing the fully unsteady pressure fields corresponding to a time-series of 2D or 3D velocity fields and solid interfaces [7].

The first test case examined for this project was an array of 3 by 3 swimmers, whose kinematics were described in the previous sections, spaced a distance of  $L$  from head to tail in the longitudinal direction and spaced a distance of either  $w = 0.3L, w = 0.4L, w = 0.7L$  or  $w = L$  in the longitudinal direction. This was simulated for 4 seconds at intervals of 0.01 seconds. For each time step, a 120 by 240 grid of velocity (corresponding to a spatial resolution of roughly  $L/40$ ) each pointing in the direction of the swimmers at constant velocity  $U_0$ , was used to compute the unsteady pressure. The Reynolds number used was 50000 for these simulations, so the algorithm disregards viscous effects. These cases were designed to mimic the 3D simulations done by Daghooghi and Borazjani and see if similar vortex shedding patterns could be observed.

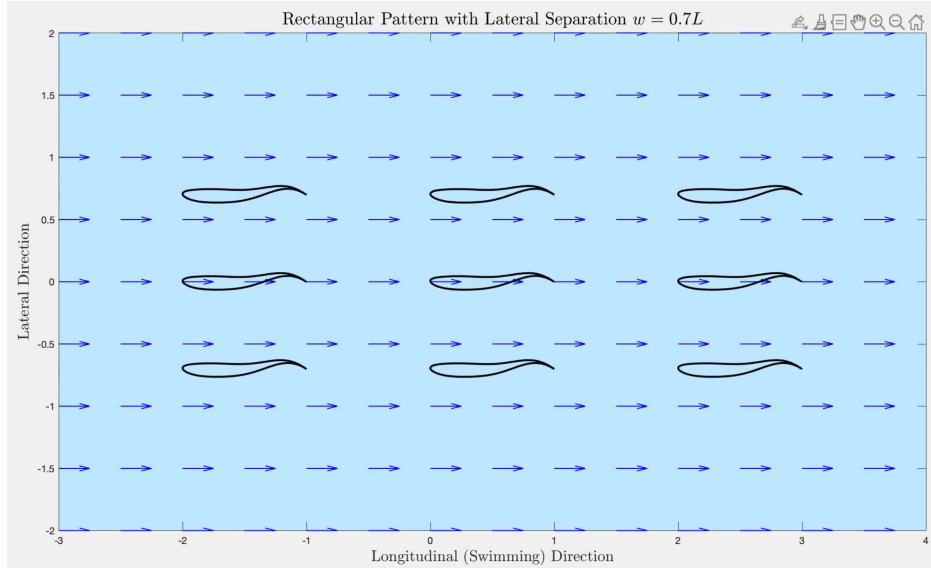


Figure 1: Inputs for rectangular pattern of swimmers, lateral distance  $w = 0.7L$

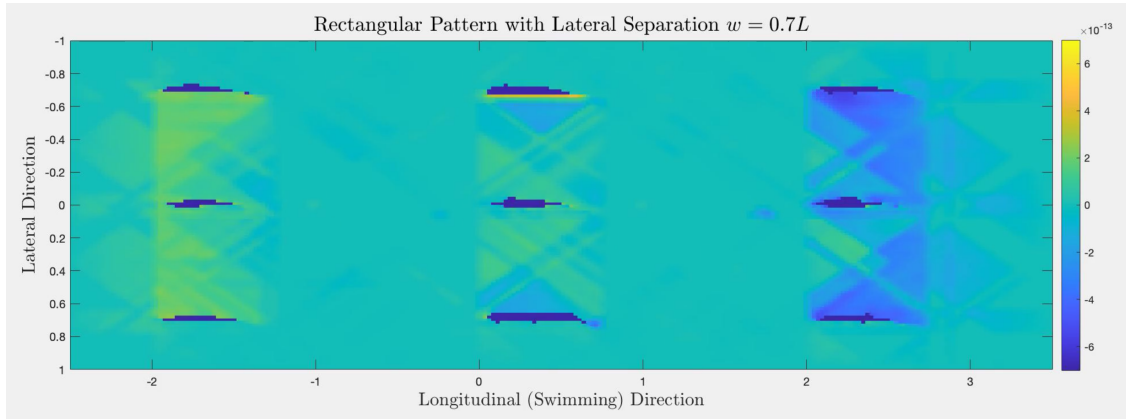


Figure 2: Pressure field for rectangular pattern of swimmers, lateral distance  $w = 0.7L$

The first figure above shows the fish boundaries and velocity field for the rectangular pattern of swimmers with lateral separation  $w = 0.7L$  at a single time instance. The figure below that shows the computed pressure field at a single time instance.

One aspect to notice is that the fish body in the output is smaller than the input. This happened for each simulation because the function used to define the body does not include boundary values, only interior values. This impacts the simulation because the body is much thinner, and the thinnest part of the fish, the tail, is getting cut-off. The tail is where the amplitude of the wave propagation through the fish is the largest and which generates the most thrust.

Also notice that we cannot see vortex shedding in the wake. A few attempts were made to fix this by increasing the spatial and time resolution, but the wake looked similar in each case. In prior studies of fish swimming conducted using the queen 2.0 algorithm, the velocity fields were found experimentally using particle image velocimetry (PIV) measurements [7] [8], whereas the velocity was assumed to be uniform for this project. The hope was that a rough estimate of the velocity field would still allow one to see a vortex shedding pattern in the pressure field, but it appears that it is not the case.

The second test case examined was a single swimmer with the pressure field first evaluated neglecting viscous effects and then evaluated accounting for viscous effects. This was also simulated at 4 seconds at intervals of 0.01 seconds and with a constant velocity vector field, but with a 128 by 128 vector field grid. These cases done to verify the assumption that viscous effects can be neglected at very large Reynolds numbers by comparing the wake cause.

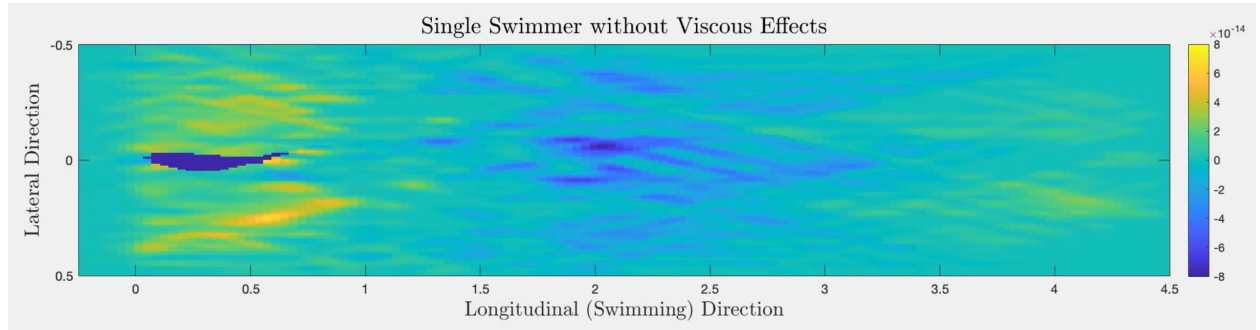


Figure 3: Pressure field for single swimmer without viscous effects

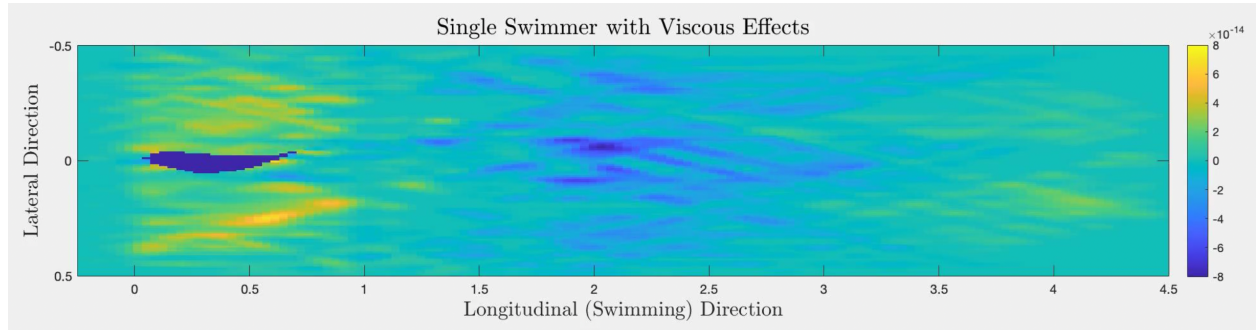


Figure 4: Pressure field for single swimmer with viscous effects

Similar to the rectangular pattern of swimmers, the swimmer is smaller than initially defined, and the pressure field fails to show vortex shedding in the wake of the swimmer. For a single swimmer, the pressure field generated with and without viscous effects are nearly identically, which helps verify the assumption made about the high Reynolds number.

## Conclusions

Using the Lighthill model, the power due to thrust was on the same order of magnitude as the power found numerically, which was expected. The Froude efficiency, however, was much twice as large as the efficiency found numerically. This was unexpected because schooling has been found to improve efficiency and because the efficiency found numerically was less than 0.5, which is not a physical result.

The pressure field visualization did not work as well as expected because the velocity field was not accurate and because the geometry of the solid surface got altered by the algorithm. In the future, it would be better to use a flow solver that computes the flow velocity or to use a flow velocity found experimentally. Additionally, when using this algorithm, the body should be made slightly larger than needed to account for the reduction in size that occurs.

**To see the code used for analytical computations and data generation and for the full video outputs generated by queen 2.0, see this GitHub repository.**

## References

- [1] M. Daghooghi and I. Borazjani, “The hydrodynamic advantages of synchronized swimming in a rectangular pattern,” *Bioinspiration & Biomimetics*, vol. 10, p. 056018, Oct. 2015.
- [2] M. J. Lighthill, “Note on the swimming of slender fish,” *Journal of Fluid Mechanics*, vol. 9, pp. 305–317, Oct. 1960.
- [3] K. N. Lucas, G. V. Lauder, and E. D. Tytell, “Airfoil-like mechanics generate thrust on the anterior body of swimming fishes,” *Proceedings of the National Academy of Sciences*, vol. 117, pp. 10585–10592, Apr. 2020.
- [4] T. Benson and T. Benson, “Interactive educational tool for classical airfoil theory,” in *35th Aerospace Sciences Meeting and Exhibit*, American Institute of Aeronautics and Astronautics, Jan. 1997.
- [5] A. Gilmanov and F. Sotiropoulos, “A hybrid cartesian/immersed boundary method for simulating flows with 3d, geometrically complex, moving bodies,” *Journal of Computational Physics*, vol. 207, pp. 457–492, Aug. 2005.
- [6] G. V. Lauder and E. D. Tytell, *Hydrodynamics of Undulatory Propulsion*. Elsevier, 2005.
- [7] J. O. Dabiri, S. Bose, B. J. Gemmell, S. P. Colin, and J. H. Costello, “An algorithm to estimate unsteady and quasi-steady pressure fields from velocity field measurements,” *Journal of Experimental Biology*, Jan. 2013.
- [8] K. N. Lucas, J. O. Dabiri, and G. V. Lauder, “A pressure-based force and torque prediction technique for the study of fish-like swimming,” *PLOS ONE*, vol. 12, p. e0189225, Dec. 2017.